0038-075C/03/16801-3–14
Soil Science

January 2003
Vol. 168, No. 1
Printed in U.S.A.

TECHNICAL ARTICLES

ANALYSIS OF UNSATURATED WATER FLOW IN A LARGE SAND TANK

Britta Schmalz[1], Bernd Lennartz[2], and Martinus Th. van Genuchten[3]

A realistic, physically based simulation of water and solute movement in the unsaturated soil zone requires reasonable estimates of the water retention and unsaturated hydraulic conductivity functions. A variety of studies have revealed the importance of how these unsaturated soil parameters are assessed and subsequently distributed over the numerical mesh on modeling outcome. This study was initiated to acquire experimental data about the water flow characteristics of sandy soils to serve as a base for numerical analyses. Specific objectives were to clarify the effects of (i) the invoked procedure for estimating the soil hydraulic parameters and (ii) using increasingly refined spatial definitions of the hydraulic properties on simulated two dimensional water content and flow velocity distributions.

Water flow in and drainage from a large sand tank (approximately 5 × 3 m^2 at the base, 6 × 5.6 m^2 at the top) was investigated using soil hydrologic and geophysical methods. Numerical analyses of variably saturated flow along a two-dimensional cross-section were carried out in attempts to describe the heterogeneous flow fields using the Richards equation-based HYDRUS-2D code. The unsaturated soil hydraulic properties were described using van Genuchten-Mualem type expressions. Information from both *in situ* and laboratory measurements was employed to obtain parameter estimates.

The observed variability in discharge rate with time was reproduced best when an average water retention curve was used and the saturated water content was set equal to the porosity, whereas cumulative outflow was predicted best when all van Genuchten hydraulic parameters were fitted to the retention data. Using heterogeneously distributed hydraulic parameters (assuming a layered profile or a random distribution of the saturated hydraulic conductivity) improve neither predictions of the cumulative discharge rate nor the variability in the outflow rate when compared with the homogeneous case. Efforts to construct or numerically simulate heterogeneous flow experiments may, therefore, not always be justified when water flow in sandy substrates is studied. (Soil Science 2003;168:3–14)

Key words: Parameter estimation, modeling, flux field variability, soil water content.

[1]Institute of Water Management and Landscape Ecology, University Kiel, Olshausenstr. 40, 24118 Kiel, Germany.

[2]Institute of Soil Science and Plant Nutrition, University Rostock, Justus-von-Liebig-Weg 6, 18051 Rostock, Germany. E-mail: bernd.lennartz@auf.uni-rostock.de

[3]George E. Brown, Jr. Salinity Laboratory, USDA, ARS, 450 West Big Springs Rd., Riverside, CA 92507-4617,

Received Feb. 27, 2002; accepted Sept. 4, 2002.

DOI: 10.1097/01.ss.0000049727.63732.8a

INFORMATION about soil hydraulic properties is needed for predicting and modeling water and solute movement in the unsaturated zone of soils. The use of deterministic models presumes having reasonable estimates of water retention and unsaturated hydraulic conductivity functions. Numerous field and laboratory methods have been developed for estimating unsaturated soil hydraulic properties. Kool et al. (1987) and Hopmans and Simunek (1999) gave overviews of parameter estimation techniques, and Feddes et al. (1988) discussed data needs for model input and validation.

One popular approach has been to use relatively simple analytical expressions for the hydraulic properties, such as the van Genuchten-Mualem equations (van Genuchten 1980). Observed field and/or laboratory soil hydraulic data are often used to derive parameters in these expressions by employing some type of fitting procedure. Direct, indirect, or inverse methods may be used for this purpose. Independently determined parameters such as saturated hydraulic conductivity, K_s, can then be used as fixed values during the optimization. Depending on the type of application, accurate estimates of the saturated, θ_s, and residual, θ_r, water contents may also be needed.

Wessolek et al. (1994) distinguished among six optimization procedures for estimating van Genuchten hydraulic parameters from observed water retention and hydraulic conductivity data. They selected different values for K_s and also for θ_s, which was assumed to be equal to porosity. The value of θ_r was set equal to zero in all runs. A reasonably good description of the hydraulic data was obtained when setting the residual water content to zero and the pore connectivity factor, l, to 0.5. A poor fit resulted when the saturated water content was equated to the porosity and K_s to its independently measured value. Bohne et al. (1997) used both simultaneous and separate fitting options to obtain the van Genuchten parameters. They found that having good data in the near-saturation range is a prerequisite for obtaining reliable parameter sets. Kablan et al. (1989) set θ_s equal to the largest single measured water content and found that the maximum water content was only approximately 70% of the estimated porosity. Using multistep outflow data, van Dam et al. (1994) studied the effect of increasing the number of optimized parameters from three to five in the optimization. Durner (1994) discussed the role of θ_r and θ_s, particularly for hydraulic conductivity predictions. He presented an example where the measured value of θ at a pressure head, h, of -1 cm was taken as θ_s. Bohne et al. (1993), among many others, treated θ_s and θ_r as unknown parameters. To avoid unrealistic results for θ_s, they used the laboratory measured 'saturated' water content at a pressure head of -2 cm as an experimental point. Further discussions of the empirical nature of θ_s and θ_r are given by Luckner et al. (1989, 1991) and Nimmo (1991). Hopmans and Overmars (1986) mentioned that, in practice, θ_r is the water content at some large negative value of the soil-water pressure head. Because no data were available in the dry range of the soil water characteristic, they fixed θ_r to its minimum value of zero. Additional discussions of θ_r are given by Russo et al. (1991), Simunek and van Genuchten (1996), and Simunek et al. (1998) among others.

In performing parameter optimizations, an important question is how well defined a fitted parameter set can or must be. Carrera and Neuman (1986) defined the terms uniqueness, identifiability, and stability in efforts to analyze the extent to which inverse problems are well posed. Many studies (e.g., Kool et al., 1987; Abbaspour et al., 1997; Hopmans and Simunek 1999) have raised concerns over the difficulties that may be encountered when trying to obtain unique inverse solutions for unsaturated flow, with several offering suggestions on how to reduce the problem of uniqueness and the minimum amount of information needed to guarantee a unique solution.

The uniqueness problem has often been analyzed by studying the behavior of parameter response surfaces. Bohne et al. (1993, 1997) and Russo et al. (1991) examined infiltration data in this manner. Tension disc infiltrometer data were similarly investigated by Simunek and van Genuchten (1996, 1997). In other studies, Toorman et al. (1992), van Dam et al. (1994), and Eching et al. (1994) analyzed one-step and multi-step outflow experiments, whereas Simunek et al. (1998) evaluated evaporation experiments from the perspective of parameter uniqueness and minimum data needs.

Field-scale unsaturated flow is further complicated by the problem of soil heterogeneity. Soil heterogeneity and the corresponding variability in soil hydraulic properties can be considered by accounting explicitly for the spatial distribution of the parameters or by using effective parameters. A variety of statistical, geostatistical, and stochastic approaches have been used for this purpose. Using two-dimensional numerical simulations, Roth (1995) found that in macroscopi-

cally homogeneous but microscopically heterogeneous media, water moved primarily through a complex network of flow channels. The hydraulic structure of the medium was characterized by two states, depending on the degree of saturation. Results showed that the spatial structure of the scaling factor of the presumed Miller-similar medium (Miller and Miller 1956) was in excellent agreement with the structure of hydraulic variables but not with that of the water flux. Polmann et al. (1991) compared tension and water content distributions obtained using both stochastic and deterministic approaches. The stochastic theory predicted less vertical flow and somewhat more horizontal spreading than a comparable deterministic analysis as a consequence of the tension-dependent anisotropy of the effective conductivity function. The heterogeneous tension contours from the detailed simulation revealed significant lateral spreading of the wetting front in both horizontal and vertical directions. Differences between the two approaches, however, were too small to indicate which one provided a better fit to the data generated in the detailed three-dimensional simulation. These differences are expected to increase over time, particularly in relatively dry situations when the effects of tension-dependent anisotropy should be larger.

Russo et al. (1994) studied how the degree of water saturation may affect solute transport in a heterogeneous soil profile. Simulation results suggested that lower saturations enhance solute spreading. The velocity field, and, hence, the spreading of the solute body, were affected greatly by the imposed flow boundary conditions at the soil surface. Quasi steady-state flow produced essentially unidirectional vertical flow, with solute spreading occurring mainly in the longitudinal direction. During transient flow, however, the flow pattern was much more complicated and essentially two-dimensional, thereby enhancing transverse spreading. In a numerical study of water flow and solute transport in a strongly heterogeneous medium having different saturation scenarios and random fields, Birkholzer and Tsang (1997) compared two-dimensional vertical cross-sections of saturation and effective permeability. They found that the solute traveled along preferred flow paths or channels. The degree of channeling, the location of channels, and the hydraulic properties along the channels, were found to be a function of the mean saturation of the flow domain. The hydraulic properties of the channels seemed to be invariant of the actual location and geometry, thus indicating that they may be an intrinsic characteristic of soil heterogeneity and degree of saturation. Kasteel et al. (2000) predicted effective water flow and solute transport behavior at the column scale by taking into account the three-dimensional structure of the hydraulic properties at the local scale. They determined the local scale hydraulic properties and the parameter structure independently and obtained good agreement between measurements and simulated pressure head and water content distributions.

The above studies reflect the importance of the way in which unsaturated soil parameters are estimated and subsequently distributed over a soil profile. To gain further insight into this problem, we analyzed, in this study, a large database of information obtained during infiltration in a large sand tank. Specific objectives of the study were:

1. To estimate the soil hydraulic properties from experimental data and to test different fitting procedures, including the effect of using different methods for estimating θ_s.
2. To evaluate the influence of geometry and boundary conditions of the experimental set-up on the unsaturated flow field.
3. To investigate the effect of using different soil hydraulic data sets and different spatial distributions of the soil hydraulic properties on two-dimensional simulation results. We were especially interested in studying the effects of using increasingly refined spatial definitions of the hydraulic properties on simulated water contents and flow velocities

MATERIALS AND METHODS

Experimental Set-up

Infiltration experiments were carried out using a large physical sand model having a base of 5 m $\times$ 3 m and a surface of 6 m $\times$ 5.6 m and containing three sloped side walls as shown in Fig. 1. The chosen construction with three sloped side walls resulted from statistical constraints. All soil hydraulic measuring devices were installed from the vertical wall. The tank was filled with a 2-m layer of homogeneous sand (Hagrey et al. 1999). Measurements of the pressure head (two vertical tensiometer profiles) and the water content (one vertical TDR profile) were conducted at eight depths. All TDR probes (IMKO systems) were calibrated before installation using the substrate of the sand tank. Estimated accuracy was 1 Vol%. A three-dimensional view of the sand tank pack-

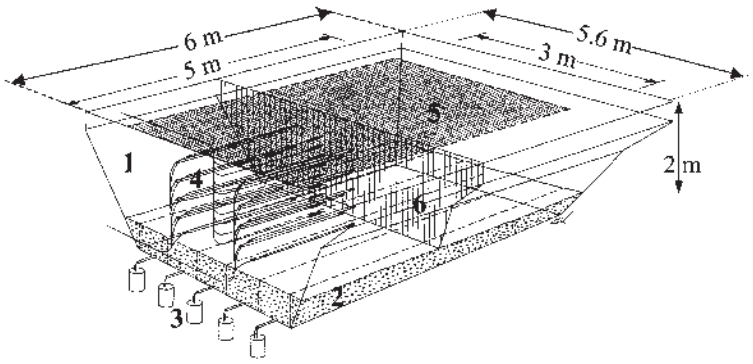

Fig. 1. Experimental set-up of the sand tank: (1) vertical (access) wall, (2) drainage layer (gravel), (3) discharge registration, (4) tensiometer, TDR-sensors, (5) irrigated area, (6) cross-section.

ing was obtained by ground penetrating radar (GPR) measurements. The lower boundary was separated into five compartments to obtain information about the spatial variability of the discharge rate. An irrigation system allowed different infiltration intensities to be imposed on the central part of the surface area (5 m × 3 m). A tent protected the set-up from natural rainfall. We performed 10 infiltration experiments, one of which will be discussed in this study. The selected experiment involved an irrigation of 4300 L (287 mm) over 14 h, which produced a total discharge of 3154 L (197 mm) over a 14-day period.

Parameter Estimation

The saturated hydraulic conductivity was calculated from the grain-size distribution of the sand according to the empirical relationship of Hazen (Hölting 1996):

$$K_s = 41.76\,(d_{10})^2 \qquad (1)$$

where K_s is given in mh^{-1}, and d_{10} is the diameter of soil particles (in mm) at 10% of the cumulative grain size distribution. The equation is presumably valid for a temperature of 10 °C.

The grain-size distribution was measured every 10 cm along three vertical profiles as well as along two horizontal profiles (25 and 30 samples, respectively). Results revealed that the texture of the sand varied slightly with depth. From the top to a depth of 70 cm, the profile was dominated by medium sand (0.2–0.63 mm), whereas fine sand (0.063–0.2 mm) dominated from 70 cm down to the bottom of the tank. The saturated hydraulic conductivity estimated using Equation (1) was found to be 0.47 m h^{-1} (with a standard deviation (SD) of 0.07 m h^{-1}) for the upper part and 0.30 m h^{-1} (SD 0.03 m h^{-1}) for the lower part. The mean hydraulic conductivity of the entire profile was 0.36 m h^{-1} (SD = 0.09 m h^{-1}). The mean bulk density measured at different depths (every 20 cm, 25 to 30 samples at each depth) was 1.48 g cm^{-3} with a SD of 0.04 g cm^{-3}.

Soil water retention functions were derived from pressure head and water content data measured in the sand tank during the infiltration experiments at eight depths (20, 40, 60, 100, 120, 140, 160, 180 cm). The retention data were described with the van Genuchten-Mualem equations (van Genuchten, 1980) as follows:

$$\theta(h) = \theta_r + \frac{\theta_s - \theta_r}{[1 + |\alpha h|^n]^m} \qquad h<0 \quad (2)$$

$$\theta(h) = \theta_s \qquad h\geq 0 \quad (3)$$

$$K(h) = K_s S_e^l\,[1-(1-S_e^{1/m})^m]^2 \qquad (4)$$

where θ is the volumetric water content, h is the pressure head, α, n, m (= 1–1/n), and l (= 0.5) are empirical parameters, S_e = (θ-θ_r)/(θ_s-θ_r) is the degree of saturation, θ_r, θ_s and K_s as defined previously.

The drying branches of the in-tank measured θ(h) data points were analyzed using two methods. For Method A, all unknown hydraulic parameters (i.e., θ_r, θ_s, α, and n) in Eqs. 2 and 3 were allowed to be adjustable. The parameters were fitted using the RETC parameter estimation code of van Genuchten et al. (1991). For Method B, θ_r and θ_s were held constant during the fitting procedure. For this purpose, θ_r was set equal to 0,

and θ_s was set equal to the porosity as calculated from the mean bulk density at each depth and the particle density (assumed as 2.65 g cm^{-3}) using the equation

$$\varepsilon = 1 - \rho_b \rho_s^{-1} \quad (5)$$

where ϵ is the porosity, ρ_b the bulk density, and ρ_s the particle density.

Numerical Experiments

Numerical experiments were subsequently conducted using the Hydrus-2D software package of Simunek et al. (1996) to obtain two-dimensional views of the infiltration and redistribution process. The windows-based Hydrus-2D package solves the Richards equation for variably saturated flow numerically, assuming applicability of the van Genuchten-Mualem soil hydraulic functions.

Because of the geometric features of the sand tank (Fig. 1), only flow in one particular cross-section was considered. To run Hydrus-2D, we implemented a relatively fine numerical mesh involving 4488 nodes depicting the geometry of the sand tank. An atmospheric boundary condition accounting for infiltration and evaporation was imposed at the soil surface, whereas a seepage face was used at the bottom boundary between the sand and a gravel drainage layer.

We conducted the following simulation runs using soil hydraulic parameter data sets of increasing complexity:

- *Homogeneous soil profile:* At first we used the measured and optimized data (Table 1) to simulate water flow in a homogeneous soil. Because the retention curves varied with depth, three data sets were selected for a more detailed investigation: the parameters for depths of 60 cm (referred to as A1 and B1), 100 cm (A2 and B2), and 140 cm (A3 and B3). One mean K_s-value (0.36 mh^{-1}) was used for these scenarios.
- *Layered soil profile:* The GPR measurements revealed the presence of a layered system (Fig. 2), apparantly caused by the method in which the tank was packed with sand. This layering was considered in simulation runs (A4; B4) by setting up a multi-layered distribution of the soil hydraulic parameters as measured at eight depths (Table 1), but assuming a two-layered distribution of K_s as determined from the measured grain-size distributions.
- *Random distribution of K_s:* Water contents and pressure heads were measured only at selected locations (two profiles), which did not allow us to fully characterize their variability in space. In contrast, bulk densities, and grain-size distributions were analyzed for each layer and included 25–30 samples per layer. Standard geostatistical analyses showed that these properties were not spatially autocorrelated. Based on this result, we simulated the flow experiment (cases A5 and B5) assuming a random K_s distribution without spatial dependency and using van Genuchten hydraulic parameters as derived from the eight measured $\theta(h)$-relationships (Table 1).
- *Inverse solution*: We also carried out a complete inverse analysis with Hydrus-2D using as our objective function the sum of squared differences between measured and simulated average discharge rates. For this scenario we again assumed a two-layered profile with different K_s-

TABLE 1

Optimized van Genuchten parameters for Method A (θ_r, θ_s, α and n variable) and Method B (θ_r=0 and θ_s=ϵ [$m^3\,m^{-3}$]

Parameters	Method	Depth [cm]							
		20	40	60	100	120	140	160	180
θ_r [m^3m^{-3}]	A	0	0	0	0	0	0	0	0
θ_s [m^3m^{-3}]	A	0.35	0.27	0.35	0.27	0.27	0.29	0.36	0.32
α [m^{-1}]	A	2.71	3.51	2.96	2.20	1.65	2.51	2.30	1.97
n [−]	A	3.60	2.55	2.66	2.96	3.55	3.28	2.63	2.96
r^2	A	0.99	1.0	0.99	1.0	1.0	0.99	0.99	1.0
θ_s [m^3m^{-3}]	B	0.45	0.45	0.43	0.44	0.45	0.46	0.45	0.45
α [m^{-1}]	B	3.22	8.19	3.88	5.64	4.28	5.35	3.07	5.77
n [−]	B	3.37	2.02	2.43	2.03	2.03	2.21	2.37	1.63
r^2	B	0.99	0.97	0.99	0.96	0.95	0.96	0.99	0.98

θ_r and θ_s are the residual and saturated water content, α and n are the van Genuchten parameters, r^2 is the coefficient of determination, ϵ is the porosity.

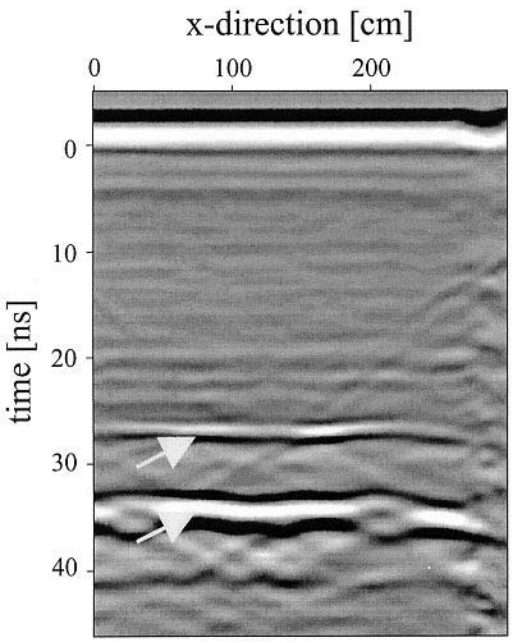

Fig. 2. Nonmigrated ground penetrating radargram: Pre-infiltration (upper arrow: electrode grid in 2-m depth not reported in this paper; lower arrow: concrete bottom of the sand tank; Hagrey et al., 1999). The radargram indicates a layered structure of the sand.

values. Values of θ_r and K_s were fixed for these simulations. We emphasize here that the main objective of this study was to present and analyze the independently acquired database; results of the inverse analysis are given here only for comparison purposes.

In the next session we will compare measured and calculated one-dimensional and two-dimensional water content distributions and fluid fluxes densities.

RESULTS AND DISCUSSION

Soil Water Retention Function

Figure 3 shows measured and fitted water retention curves at three depths. The measured water retention data are typical of the range of results we obtained and indicate nonuniform, depth-dependent retention behavior. A comparison of the fitted van Genuchten parameters (Table 1) showed that the θ_s-values derived from porosity (Method B) were much larger than the fitted values obtained using Method A. Using the measured θ_s-values also altered the fitted retention curve near saturation significantly. In contrast, θ_r-values for all depths converged to 0 using both fitting procedures (A and B). Close examination of the fitted hydraulic parameter and visual inspection of the different retention functions did not reveal a clear separation of the soil profile into two layers as suggested by the observed grain-size distributions. As was expected (Bohne et al., 1993), coefficients of determination were slightly better when the number of parameters allowed to float during the fitting procedures was increased (Table 1).

Effective parameters obtained with the inverse solution using HYDRUS-2D are listed in Table 2. Notice that the estimated θ_s-values for the two layers compare closely with those of optimization procedure A (Table 1). The r^2 value for regression of observed versus fitted values was 1.0, indicating excellent agreement between measured and optimized values.

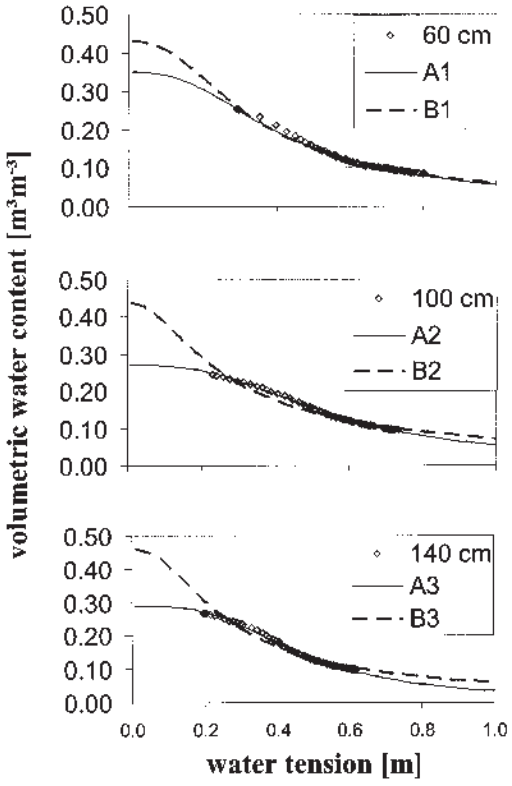

Fig. 3. Water retention curves for three selected depths and optimized values using Method A (solid lines) and B (dashed lines).

TABLE 2

Parameter sets obtained with the inverse option of HYDRUS-2D (fixed θ_r, K_s)

Layer	θ_r [$m^3\ m^{-3}$]	θ_s [$m^3\ m^{-3}$]	α [m^{-1}]	n [−]	K_s [$m\ h^{-1}$]
1	0	0.26	2.40	2.51	0.47
2	0	0.33	4.03	2.30	0.30

θ_r and θ_s are the residual and saturated water content, α and n are the van Genuchten parameters, K_s is the saturated hydraulic conductivity.

Water Flux

Darcian Fluxes at the Lower Boundary

The particular design of the sand tank made it possible for us to analyze the variability of the discharge rate in space and time. The mean flux and the corresponding coefficient of variation (CV) were computed from the five outflow compartments. Values of the CV versus time of each simulation run, along with the CVs calculated from the measured values, are given in Fig. 4. The measured discharge had a large CV (43%) initially, but it then decreased exponentially to about 14%. The two modeling approaches (A and B) produced divergent results. Although discharge rates for the A group (more darkly shaded in Fig. 4) were less variable across the lower boundary at early stages of the experiment, and more variable at later times, CVs calculated for the B-runs (lightly shaded) were more in line (especially B1) with the measured data. As expected, spatial variability in the predicted discharge rate was large when a heterogeneous soil profile (A5) was considered. Except for A1 after about 2 h, distributions versus time of the CVs of simulation runs A1–A4 were all comparable. In contrast to Method A, the CVs for the homogeneous cases B2 and B3 were larger than those for the stochastic case B5.

Flow velocity vectors illustrating the two-dimensional flux field within the sand tank and across its lower boundary are displayed in Fig. 5 and are exemplary for case A1 at 2 h after the onset of discharge. Discharge started at different times, depending on the invoked simulation approach (Table 3). Although discharge had already started during irrigation when Method A was used, it occurred after irrigation had ended (at 14 h) for the B-scenarios. The velocity vectors in Fig. 5 indicate some lateral flow into the nonirrigated side areas, from which water flowed funnel-like downward along the sloped sides of the tank.

Simulation runs for all Method B scenarios produced relatively low flow velocities in the entire sand body, primarily because irrigation had already stopped. The highest velocities occurred at the lower boundary. The velocity vectors were orientated diagonally and horizontally because of the development of a saturated zone at the lower boundary (characteristic of a seepage face) and concomitant lateral spreading.

Discharge rates were distributed relatively uniformly along the lower boundary for all simulation runs, with slightly higher fluxes in the middle of the tank and along the lower portions

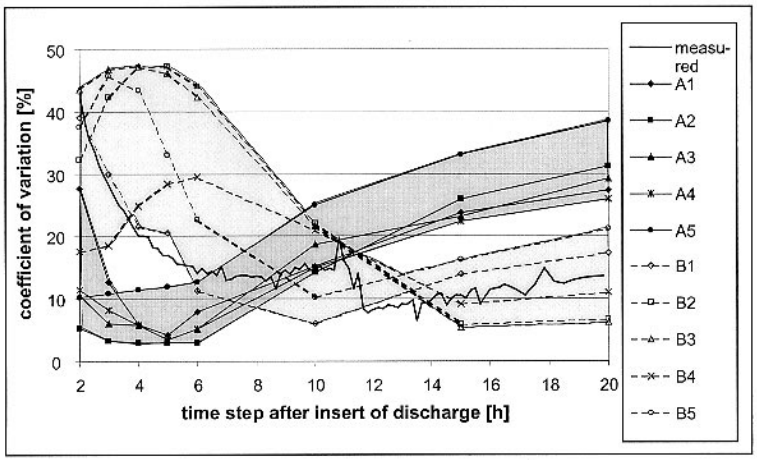

Fig. 4. Coefficient of variation of Darcian fluxes of the five compartments versus time (the CV is referring to the mean value of discharge of every compartment).

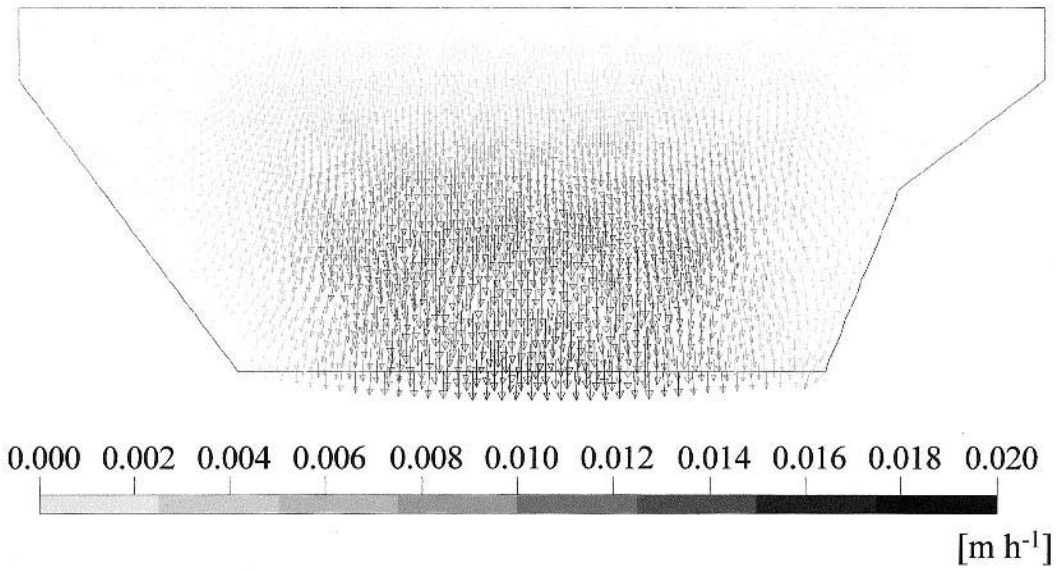

Fig. 5. Darcy's velocity vectors 2 hours after the onset of discharge in run A1 (16 h after onset of irrigation).

of the side walls. The measured fluxes were highest in the middle compartments, with velocities generally smaller than those simulated. No increases in the measured outflow rates were observed near the side walls.

Methods A and B both yielded discharge rates that were not quite identical to the measured fluxes. At the selected time (2 h after drainage started) the effect of geometry (sloped side walls) and irrigated area (nonirrigated lateral areas) was apparently higher for the simulation runs than for the experiment. Neither the magnitude of the velocity nor its distribution corresponded closely with the measured values. Method B, in particular, generated results that deviated from the observed discharge rates.

Table 4 shows results from a statistical analysis of the mean Darcian fluxes at the lower boundary 2 h after the onset of discharge. The mean fluxes of all simulation runs were greater than the measured values, while the CVs were smaller (except B3). Also, the CVs of the B-runs were generally larger than those for the A group but were fairly similar to those of the observed flux.

Cumulative Discharge

The cumulative flux was described best when a homogeneous soil profile (A1) was assumed (Fig. 6). When θ_r and θ_s were fixed at zero and the porosity, respectively (Method B), the resulting van Genuchten parameters produced cumulative outflow values that differed from the observed curves. For this case, the onset of outflow was late, and the rate (slope of curve) was always much smaller than the measured data (Table 3). This is in contrast to Wessolek et al. (1994), who found that using the porosity for θ_s increased the predicted outflow rates significantly and produced better matches with the observed values. Param-

TABLE 3

Onset of discharge and cumulative flux after 336 hours at the lower boundary of selected simulation runs (Methods A and B)

	Measured	A1	A2	A3	A4	A5
Onset of discharge [h]	13.25	14.1	8.1	11.5	11.3	9.9
Cum. flux [mm]	197.1	200.3	235.3	204.4	211.6	225.6
	Measured	B1	B2	B3	B4	B5
Onset of discharge [h]	13.25	19.9	23.8	26.4	25.1	18.7
Cum. flux [mm]	197.1	165.6	150.0	137.5	145.0	167.2

TABLE 4
Descriptive statistics of measured and calculated Darcian fluxes at the lower boundary two hours after the start of discharge in each run

	Measured	A1	A2	A3	A4	A5
mean [m h^{-1}]	0.0088	0.0139	0.0163	0.0156	0.0150	0.0163
CV [%]	43	28	5	10	11	10
min [m h^{-1}]	0.0041	0.0077	0.0151	0.0129	0.0124	0.0141
max [m h^{-1}]	0.0149	0.0183	0.0177	0.0178	0.0175	0.0184
	Measured	B1	B2	B3	B4	B5
mean [m h^{-1}]	0.0088	0.0158	0.0185	0.0186	0.0107	0.0239
CV [%]	43	39	32	44	18	38
min [m h^{-1}]	0.0041	0.0097	0.0088	0.0063	0.0073	0.0132
max [m h^{-1}]	0.0149	0.0253	0.0249	0.0278	0.0127	0.0393

CV is the coefficient of variation ($n = 5$).

eter sets derived using Method A yielded flow scenarios that over-predicted the measured discharge rate. Our results obtained using both Method A and Method B indicate the importance of having good estimates of θ_s and confirm similar findings by Bohne et al. (1993, 1997).

Compared with the three homogeneous cases, the layered soil profile (A4, B4) resulted in slightly lower fluxes. Fluxes for the layered profile were also lower compared with cases (A5, B5) that used a random distribution of the soil saturated hydraulic conductivity. Results obtained with the latter two simulations (A5, B5) were within the range of cumulative fluxes computed for the homogeneous soil profiles.

Water Content Distributions

Two-dimensional cross-sections of simulated water content distributions 12 h after the onset of irrigation are depicted in Fig. 7. All 10 simulation runs show similar features: relatively high water contents in the central part of the tank and at the lower boundary, and lower water contents at the sides. This was expected since only the central part of the physical model was irrigated. The sloped side walls generated a funnel-like flow regime that resulted in slightly higher water contents at and near the lower boundary.

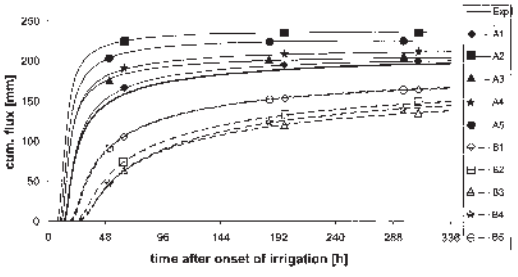

Fig. 6. Cumulative boundary flux of selected simulation runs.

The different scenarios produced an interesting range of flow situations. The layered structure (A4, B4) caused discontinuities in the water content across layer boundaries, as well as some lateral flow along these boundaries (especially near the dry areas). As expected, the simulations with a stochastic distribution of K_s (A5, B5) generated a random structure of the water content (Fig. 5, bottom) as a consequence of local heterogeneity. These results are consistent with those of Roth (1995) and Hammel and Roth (1998) who noticed the development of flow channels. In addition, Birkholzer and Tsang (1997) found that the flow patterns, ranging from relatively homogeneous patterns to strong channeling effects, were saturation dependent.

For comparison purposes we analyzed statistically (descriptive statistics) the water content cross-sections of the irrigated central part of the sand tank at a depth of 60 cm. Results are shown in Table 5. Compared with the measured water content in the center part of the tank (0.25 m^3m^{-3}), Method A generally gave much lower values (means of 0.13 to 0.19 m^3m^{-3}), whereas Method B simulation generated results that were much more in line with the observed values (means of 0.23 to 0.28 m^3m^{-3}). The calculated wetting fronts at that time (12 h) had reached different depths for the various simulation runs.

The CVs in Table 5 indicate considerable variability in the water content for the simulations, assuming a random K_s distribution (A5, B5) estimated from the measured bulk densities and

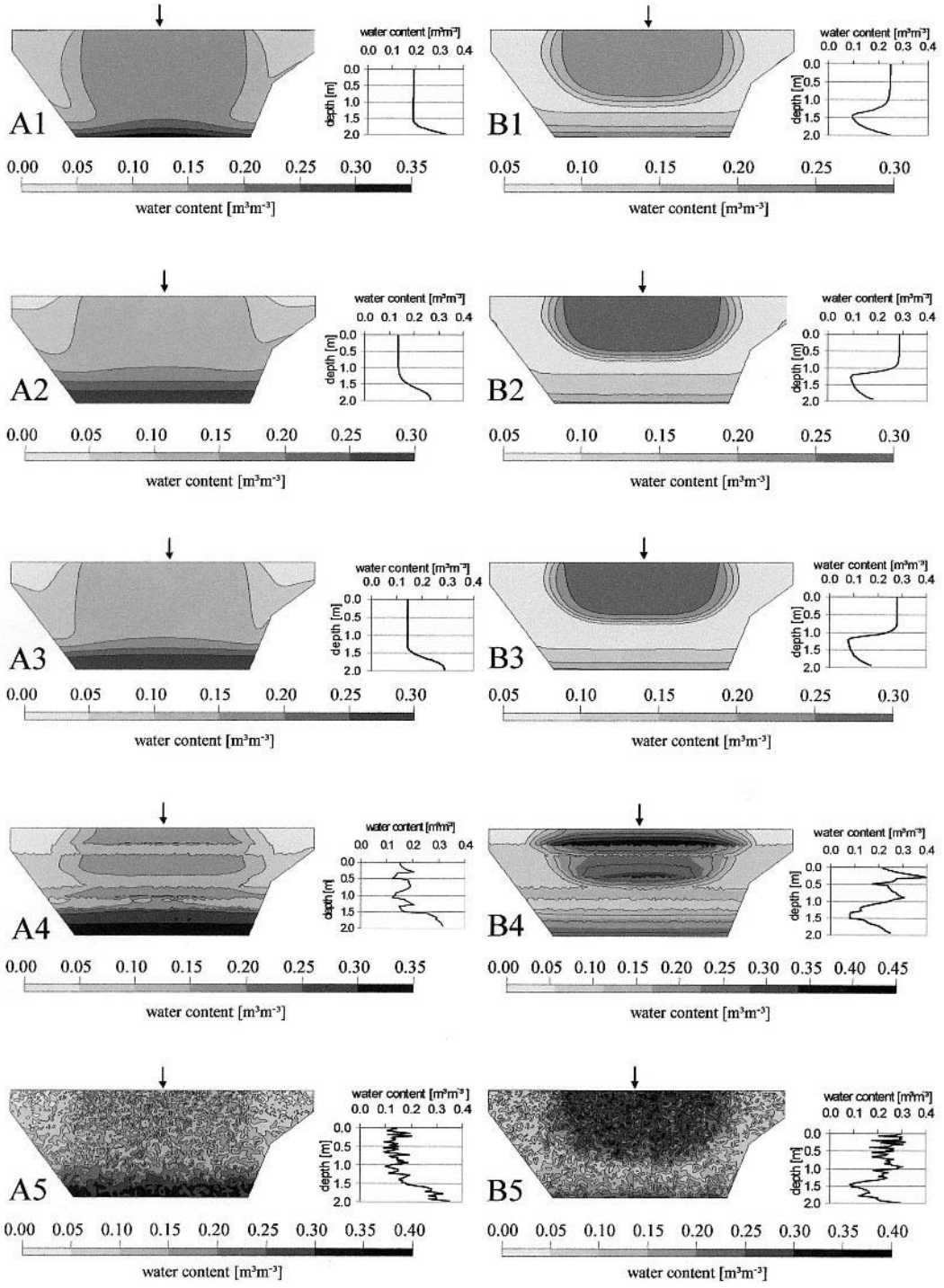

Fig. 7. Distribution of water content 12 h after onset of irrigation: Two-dimensional cross-sections and one-dimensional vertical profiles (arrows show position of vertical profile; note: different scaling to show an optimal resolution for each section).

TABLE 5

Descriptive statistics of the observed water contents at 60 cm depth in the central part of the tank 12 hours after onset of irrigation (n = 163)

	A1	A2	A3	A4	A5	B1	B2	B3	B4	B5
mean [m^3m^{-3}]	0.19	0.13	0.14	0.18	0.14	0.24	0.28	0.27	0.23	0.25
CV [%]	5	5	7	5	22	6	6	7	9	15
min [m^3m^{-3}]	0.15	0.11	0.10	0.14	0.08	0.18	0.19	0.18	0.15	0.16
max [m^3m^{-3}]	0.19	0.14	0.14	0.19	0.20	0.25	0.29	0.28	0.24	0.32

CV is the coefficient of variation.

grain-size distributions. Results for these two cases most closely resembled observed values.

CONCLUSIONS

Analysis of the water fluxes and water content distributions showed that the quality of the different simulation runs depended on which parameter of the system was used as the criterion (cumulative flux, spatial variation in discharge rate, two-dimensional water content distribution, or variability). None of the simulation approaches studied reproduced both the measured water balance and the observed flow behavior exactly. From a detailed analysis of the simulation runs, the following conclusions emerged:

1. The selected optimization procedures produced different water retention parameter sets. The in-tank measured data covered only a small range of the entire water retention curve. Accordingly, the manner in which the saturated water content, θ_s, was estimated was the most critical factor affecting all other soil hydraulic parameters and, directly or indirectly, the modeled flow regime. Agreement with observed cumulative water fluxes was best when we assumed the presence of a homogeneous soil profile, used a mean water retention curve as derived from the sensors at 60 cm depth, and used optimized θ_s and θ_r values. In contrast, observed variabilities in the discharge rate with time could be reproduced reasonable well with an average water retention curve and using porosity for θ_s. This scenario also produced the most realistic range in measured water contents.
2. The geometry of the sand tank and the size of the irrigated area affected discharge generation greatly. Lateral flow into the nonirrigated areas as a result of soil water pressure head gradients was facilitated by the layered structure of the sand packing. The sloped side walls induced some lateral discharge at the lower boundary. The lower boundary (seepage face) produced a saturated zone locally, with some lateral flow and nonuniform discharge.
3. Our results demonstrated numerically the overriding effect of how the soil hydraulic properties were distributed over the soil profile (a homogeneous profile, a layered system, or a profile having a random distribution of K_s). The heterogeneous (layered or random) profiles were implemented on the basis of GPR information and in-tank measured soil physical data, assuming such heterogeneous profiles did not improve our predictions of water flow substantially. Thus, our results suggests that elaborate efforts to set up heterogeneous cases, either numerically or physically, may not always be justified when water flow in sandy substrates is to be simulated.

ACKNOWLEDGMENT

This work was supported by the German Research Foundation under grant ME 335/96–2.

REFERENCES

Abbaspour, K. C., M. Th. van Genuchten, R. Schulin, and E. Schläppi. 1997. A sequential uncertainty domain inverse procedure for estimating subsurface flow and transport parameters. Water Resour. Res. 33:1879–1892.

Birkholzer, J., and C.-F. Tsang. 1997. Solute channeling in unsaturated heterogeneous porous media. Water Resour. Res. 33:2221–2238.

Bohne, K., D. Radcliffe, G. Wessolek, and S. Zacharias. 1997. Inverse method to estimate soil hydraulic parameters from field measurements of ponded infiltration. *In* Characterization and measurement of the hydraulic properties of unsaturated porous media, Proc. Int. Workshop, Riverside, CA, Oct. 22–24, 1997, pp. 799–815.

Bohne, K., C. Roth, F. J. Leij, and M. Th. van Genuchten. 1993. Rapid method for estimating the unsaturated hydraulic conductivity from infiltration measurements. Soil Sci. 155:237–244.

Carrera, J., and S. P. Neuman. 1986. Estimation of aquifer parameters under transient and steady state

conditions: 2. Uniqueness, stability, and solution algorithms. Water Resour. Res. 22:211–227.
Durner, W. 1994. Hydraulic conductivity estimation for soils with heterogeneous pore structure. Water Resour. Res. 30:211–223.
Eching, S. O., J. W. Hopmans, and O. Wendroth. 1994. Unsaturated hydraulic conductivity from transient multistep outflow and soil water pressure head. Soil Sci. Soc. Am. J. 58:687–695.
Feddes, R. A., P. Kabat, P. J. T. van Bakel, J. J. B. Bronswijk, and J. Halbertsma. 1988. Modelling soil water dynamics in the unsaturated zone – State of the art. J. Hydrol. 100:69–111.
Hagrey, S. A. al, T. Schubert-Klempnauer, D. Wachsmuth, J. Michaelsen, and R. Meissner. 1999. Preferential flow: first results of a full-scale flow model. Geophys. J. Int. 138:643–654.
Hammel, K., and K. Roth. 1998. Approximation of asymptotic dispersivity of conservative solute in unsaturated heterogeneous media with steady state flow. Water Resour. Res. 34:709–715.
Hölting, B. 1996. Hydrogeologie. Einführung in die allgemeine und angewandte Hydrogeologie. Enke. Stuttgart.
Hopmans, J. W., and B. Overmars. 1986. Presentation and application of an analytical model to describe soil hydraulic properties. J. Hydrol. 87:135–143.
Hopmans, J. W., and J. Simunek. 1999. Review of inverse estimation of soil hydraulic properties. *In* Characterization and Measurement of the Hydraulic Properties of Unsaturated Porous Media. M. Th. van Genuchten, F. J. Leij, and L. Wu (eds.). Proc. Int. Workshop, Part 1, University of California, Riverside, CA, pp. 643–659.
Kablan, R. A. T., R. S. Mansell, S. A. Bloom, and L. C. Hammond. 1989. Determinations of unsaturated hydraulic conductivity for Candler sand. Soil Sci. 148:155–164.
Kasteel, R., H.-J. Vogel, and K. Roth. 2000. From local hydraulic properties to effective transport in soil. Eur. J. Soil Sci. 51:81–91.
Kool, J. B., J. C. Parker, and M. Th. van Genuchten. 1987. Parameter estimation for unsaturated flow and transport models–A review. J. Hydrol. 91:255–293.
Luckner, L., M. Th. van Genuchten, and D. R. Nielsen. 1989. A consistent set of parametric models for the two-phase flow of immiscible fluids in the subsurface. Water Resour. Res. 25:2187–2193.
Luckner, L., M. Th. van Genuchten, and D. R. Nielsen. 1991. Reply. Water Resour. Res. 27:663–664.
Miller, E. E., and R. D. Miller. 1956. Physical theory for capillary flow phenomena. J. Appl. Phys. 27:324–332.
Nimmo, J. R. 1991. Comment on the treatment of residual water content. *In* A Consistent Set of Parametric Models for the Two-Phase Flow of Immiscible Fluids in the Subsurface. L. Luckner et al. Water Resour. Res. 27:661–662.
Polmann, D. J., D. McLaughlin, S. Luis, L. W. Gelhar, and R. Ababou. 1991. Stochastic modeling of large-scale flow in heterogeneous unsaturated soils. Water Resour. Res. 27:1147–1458.
Roth, K. 1995. Steady state flow in an unsaturated, two-dimensional, macroscopically homogeneous, Miller-similar medium. Water Resour. Res. 31: 2127–2140.
Russo, D., E. Bresler, U. Shani, and J. C. Parker. 1991. Analyses of infiltration events in relation to determining soil hydraulic properties by inverse problem methodology. Water Resour. Res. 27:1361–1373.
Russo, D., J. Zaidel, and A. Laufer. 1994. Stochastic analysis of solute transport in partially saturated heterogeneous soil. 1. Numerical experiments. Water Resour. Res. 30:769–779.
Simunek, J., M. Sejna, and M. Th. van Genuchten. 1996. Hydrus-2d, Simulating Water Flow and Solute Transport in Two-Dimensional Variably Saturated Media. User's Manual. U.S. Salinity Lab., USDA/ARS, Riverside, CA.
Simunek, J., and M. Th. van Genuchten. 1996. Estimating unsaturated soil hydraulic properties from tension disc infiltrometer data by numerical inversion. Water Resour. Res. 32:2683–2696.
Simunek, J., and M. Th. van Genuchten. 1997. Estimating unsaturated soil hydraulic properties from multiple tension disc infiltrometer data. Soil Sci. 162:383–398.
Simunek, J., O. Wendroth, and M. Th. van Genuchten. 1998. Parameter estimation analysis of the evaporation method for determining soil hydraulic properties. Soil Sci. Soc. Am. J. 62:894–905.
Toorman, A. F., P. J. Wierenga, and R. G. Hills. 1992. Parameter estimation of hydraulic properties from one-step outflow data. Water Resour. Res. 28: 3021–3028.
van Dam, J. C., J. N. M. Stricker, and P. Droogers. 1994. Inverse method to determine soil hydraulic functions from multistep outflow experiments. Soil Sci. Soc. Am. J. 58:647–652.
van Genuchten, M. Th. 1980. A closed-form equation for predicting the hydraulic conductivity of unsaturated soil. Soil Sci. Soc. Am. J. 44:692–898.
van Genuchten, M. Th., F. J. Leij, and S. R. Yates. 1991. The RETC Code for quantifying the hydraulic functions of unsaturated soils. U.S. Salinity Lab., USDA/ARS, Riverside, CA.
Wessolek, G., R. Plagge, F. J. Leij, and M. Th. van Genuchten. 1994. Analysing problems in describing field and laboratory measured soil hydraulic properties. Geoderma 64:93–110.